PROCEEDINGS OF SCIENCE

Collins-Soper kernel from transverse momentum-dependent wave functions in LaMET

Min-Huan Chu[a,b,*]

[a] *INPAC, Key Laboratory for Particle Astrophysics and Cosmology (MOE), Shanghai Key Laboratory for Particle Physics and Cosmology, School of Physics and Astronomy, Shanghai Jiao Tong University, Shanghai 200240, China*

[b] *Key Laboratory for Particle Astrophysics and Cosmology (MOE), Shanghai Key Laboratory for Particle Physics and Cosmology, Tsung-Dao Lee Institute, Shanghai Jiao Tong University, Shanghai 200240, China*

E-mail: tony_chu@sjtu.edu.cn

In this work we present the analysis of Collins-Soper kernel extracted from pion transverse momentum dependent wave functions in the framework of large momentum effective theory from lattice QCD. We use clover fermion action with $2+1+1$ flavors of highly improved staggered quarks (HISQ), with lattice spacing $a = 0.12$fm and volume $L^3 \times T = 48^3 \times 64$. The results are obtained based on pion mass $M_\pi = 670$MeV, and three hadron momenta as $P^z = 2\pi/L \times \{8, 10, 12\} = \{1.72, 2.15, 2.58\}$GeV. Preliminary results are found in consistent with previous LQCD determinations and phenomenological results.

The 38th International Symposium on Lattice Field Theory, LATTICE2021 26th-30th July, 2021 Zoom/Gather@Massachusetts Institute of Technology

*Speaker

PoS(LATTICE2021)424

1. Introduction

The transverse momentum-dependent (TMD) parton distribution functions are important to describe the intrinsic transverse momentum of the partonic constituents of protons and can be accessed in inclusive high energy collisions. Transverse momentum-dependent wave functions (TMDWFs) are the most ingredient to predict physical observables. In the past few decades, there have been many detailed studies to explore the internal structure of hadrons through parton distributions from both experiments and the theory calculations in the framework of lattice QCD mainly in large momentum effective theory (LaMET) [1, 2].

Recently LaMET has made revolutionary progresses. For recent reviews, please see Refs.[3, 4]. In the mean while, TMDWFs and TMDPDFs are found calculable on the Eucledian lattice through LaMET approach [5, 6]. The rapidity evolution can also be obtained via the quasi-TMDPDFs [7] and TMDWFs [8], and quite a few papers are made on the lattice calculation [9–12, 14].

In this talk, we use the configurations based on clover fermion action with $2+1+1$ flavors of highly improved staggered quarks (HISQ) action [15], generated by MILC collaboration [16], with lattice spacing $a = 0.12$fm and volume $L^3 \times T = 48^3 \times 64$. Sea quark masses on this ensemble have been tuned to match the physical quark masses in nature [16], while the valence quark mass is chosen to match pion mass $M_\pi = 670$MeV. To achieve the infinite momentum limit with a reasonable signal, we employ three hadron momenta as $P^z = 2\pi/L \times \{8, 10, 12\} = \{1.72,\ 2.15,\ 2.58\}$GeV, which are equivalent to the boost factor $\gamma = \{2.57,\ 3.21,\ 3.85\}$.

2. Quasi-TMD Wave Function and Collins-Soper Kernel

For physical meaning, Collins-Soper kernel describes the rapidity evolution of light-cone TMDWFs $\psi^\pm(x, b_\perp, \mu, \zeta)$. The evolution equation of rapidity for the rapidity-renormalized LFWF reads [8]

$$2\zeta \frac{d}{d\zeta} \ln \psi^\pm(x, b_\perp, \mu, \zeta) = K(b_\perp, \mu). \tag{1}$$

In the large hadron momentum circumstances, the parton momentum-dependence of the quasi-TMDWFs should be

$$P^z \frac{d}{dP^z} \ln \tilde{\psi}^\pm(x, b_\perp, \mu, \zeta) = K(b_\perp, \mu) + \sum_i \frac{1}{2} \mathcal{G}^\pm(x_i^2 \zeta_z, \mu) + O(1/P^z)^2, \tag{2}$$

where $\zeta_z = 4x^2(P^z)^2$. Except for Collin-Soper kernel $K(b_\perp, \mu)$ terms, the evolution equation of quasi-TMDWFs $\tilde{\psi}^\pm(x, b_\perp, \mu, \zeta)$ still includes a perturbative part $\mathcal{G}^\pm(x_i^2 \zeta_z, \mu)$, and the higher power terms of $(1/P^z)^2$ are omitted.

In LaMET, by using the matching formula between quasi-TMDWFs and light-cone ones, we determine Collins-Soper kernel $K(b_\perp, \mu)$ by the ratio of quasi-TMDWFs $\tilde{\psi}(x, b_\perp, \mu, \zeta_z)$ at different hadron momenta (taken in z-direction) $P^z >> \Lambda_{\rm QCD}$[8]:

$$K(b_\perp, \mu) = \frac{1}{2}\left(\frac{2}{\ln(\zeta_z/\zeta_z')} \frac{H_N^+(\zeta_z')\tilde{\psi}_N^+(x_i, b_\perp, \mu, \zeta_z)}{H_N^+(\zeta_z)\tilde{\psi}_N^+(x_i, b_\perp, \mu, \zeta_z')} + \frac{2}{\ln(\zeta_z/\zeta_z')} \frac{H_N^-(\zeta_z')\tilde{\psi}_N^-(x_i, b_\perp, \mu, \zeta_z)}{H_N^-(\zeta_z)\tilde{\psi}_N^-(x_i, b_\perp, \mu, \zeta_z')} \right), \tag{3}$$

with the H_N^+ corresponding to the one-loop perturbative hard function[8],

$$H_1^{\pm}(\zeta_z) = 1 + \alpha_s \frac{C_F}{4\pi}\left(-\frac{5\pi^2}{6} - 4 + \ell_{\pm} + \bar{\ell}_{\pm} - \frac{1}{2}(\ell_{\pm}^2 + \bar{\ell}_{\pm}^2)\right), \tag{4}$$

where $\ell_{\pm} = \ln(-\zeta_z \pm i\epsilon) - \ln\mu^2$, and $\bar{\ell}_{\pm} = \ln(-\bar{\zeta}_z \pm i\epsilon) - \ln\mu^2$. $\zeta_z = (2xP\cdot n_z)^2$ and $\bar{\zeta}_z = (2\bar{x}P\cdot n_z)^2$. This matching kernel relates a multiplicative factorization between quasi-TMDWFs and light-cone TMDWFs.

Quasi-TMDWF for a pseudoscalar meson like pion is defined as:

$$\tilde{\psi}^{\pm}(x, b_\perp, \mu, \zeta^z) = \lim_{L\to\infty} \int \frac{P^z dz}{4\pi} e^{i(x-1/2)P^z z} \frac{1}{\sqrt{Z_E(2L, b_\perp, \mu)}} \tilde{\psi}_l^{\pm}(z, b_\perp, \zeta^z), \tag{5}$$

where $\zeta^z = 2xP^z n^z$ denotes the z-direction hadron momenta, and the Lorentz structure Γ can be chosen for the leading twist $\gamma^\mu\gamma_5$ in coordinate quasi-TMDWFs $\tilde{\psi}^{\pm}$. In the denominator, the renormalization factor $Z_E(2L, b_\perp, \mu)$ refers to the Wilson loop matrix element which can cancel the linear divergence in $\tilde{\Psi}$, and renormalize it into $\overline{\text{MS}}$ scheme:

$$\begin{aligned} Z_E(2L, b_\perp, \mu) &= \langle 0|\mathcal{P}\exp\int_{-L}^{L} dz A_z(0, z) + \mathcal{P}\exp\int_0^b dx A_x(L, x) + \mathcal{P}\exp\int_L^{-L} dz A_z(b, z) \\ &\quad + \mathcal{P}\exp\int_b^0 dx A_x(x, -L)|0\rangle. \end{aligned} \tag{6}$$

The connection in transverse plane of two spinor field operators for quasi-TMDWFs is needed to satisfy gauge invariance which removes the divergence in the Wilson line self energy. So the renormalization scheme is to diminish a same construction factor in the transverse plane, which should also be gauge invariant.

The quasi-TMDWFs in coordinate space are defined as a matrix element from vacuum to hadron state and computed by the ratio of non-local two point function with Wilson line between two field operators and a local one:

$$\begin{aligned} \tilde{\psi}^{\pm}(z, b_\perp, \zeta^z) &= \langle 0|\overline{\Psi}_{\mp n^z}(zn^z/2 + b_\perp)\Gamma\Psi_{\mp n^z}(-zn^z/2)|\pi\rangle = \frac{C_2(L, b_\perp, z, t, P^z)}{C_2(0, 0, 0, t, P^z)}, \\ \Psi_{\mp n^z}(-zn^z/2) &= \lim_{L\to\infty} \mathcal{P}\exp\left\{ig\int_{-zn^z/2}^{\mp Ln^z - zn^z/2} d\lambda A^z(-zn^z/2 + \lambda n^z)\right\} \times q(-zn^z/2). \end{aligned} \tag{7}$$

The Wilson lines are shown in Fig. (1). We need to construct Wilson loop matrix element $Z_E(2L, b_\perp)$ with length L and width $b_\perp$ to renormalize such a matrix element.

Two point correlation functions are generated by Coulomb gauge fixed wall source propagators with energy $E_{P^z} = \sqrt{m_\pi^2 + (P^z)^2}$:

$$\begin{aligned} C_2(L, b_\perp, z, t, P^z) &= \int d^3x d^3y e^{-i\vec{P}\vec{x} + i\vec{P}\vec{y}} \langle 0|\bar{\Psi}_{f_1}(\vec{x} + zn^z/2 + b_\perp, t)\Gamma\Psi_{f_2}(\vec{x} - zn^z/2, t) \\ &\quad \bar{\Psi}_{f_2}(\vec{y}, 0)\Gamma'\Psi_{f_1}(\vec{y}, 0)|0\rangle \\ &= \frac{L^3}{2E_{P^z}} e^{-iE_{P^z}t}\langle 0|\overline{\Psi}_{f_1}(zn^z/2 + b_\perp)\Gamma\Psi_{f_2}(-zn^z/2)|\pi(P^z)\rangle, \\ C_2(0, 0, 0, t, P^z) &= \frac{L^3}{2E_{P^z}} e^{-iE_{P^z}t}\langle 0|\overline{\Psi}_{f_1}(0)\Gamma\Psi_{f_2}(0)|\pi(P^z)\rangle. \end{aligned} \tag{8}$$

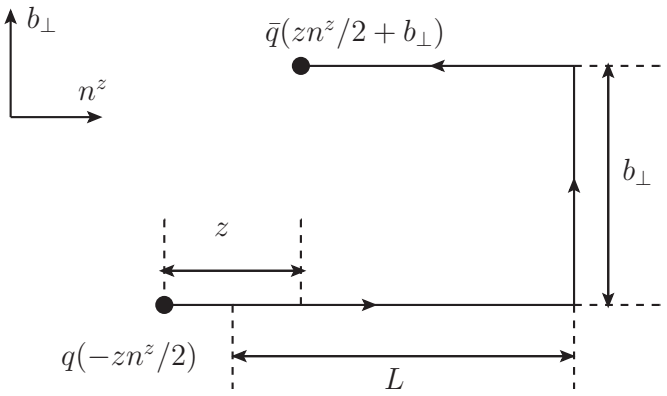

Figure 1: Diagrammatic representation of the Wilson line included in coordinate quasi-wave function.

Therefore the renormalized $\tilde{\psi}$ can be obtained as:

$$\tilde{\psi}^{\pm}(z, b_\perp, \zeta^z)_{rn} = \lim_{L\to\pm\infty} \frac{C_2(L, b_\perp, z, t, P^z)}{C_2(0, 0, 0, t, P^z)\sqrt{Z_E(2L, b_\perp)}}, \tag{9}$$

3. Numerical Results

The Lattice configurations are based on clover fermion action with 2+1+1 flavors of highly improved staggered quarks (HISQ) action [15], generated by MILC collaboration [16]. To improve the signal, the valence quark mass to make $m_\pi = 670$MeV is used. The used hardron momenta are $P^z = 2\pi/L \times \{8, 10, 12\} = \{1.72, 2.15, 2.58\}$GeV to approach the infinity momentum limit.

The quasi-TMDWFs are extracted from two point correlation functions as described in Eq. (8). As the parametrization formula behaves like exponential decay for $C_2(L, b_\perp, z, t, P^z)$ as a function of t in Eq. (11), a two-state fit is often adopted to extract quasi-TMDWFs $\tilde{\psi}^{\pm}(L, b_\perp, z, P^z)$. To make it simple, we use the notation $\tilde{\psi}(b_\perp, z, P^z)$ instead of $\tilde{\psi}^{\pm}(b_\perp, z, P^z)$,

$$C_2(0, 0, 0, t, \vec{P}) = c_0(0)e^{-Et}(1 + c_1(0)e^{-\Delta Et}), \tag{10}$$

$$\bar{C}_2(L, b_\perp, , z, t, \vec{P}) = \frac{\tilde{\psi}(L, b_\perp, z, \vec{P})(1 + c_1(L, b_\perp, z)e^{-\Delta Et})}{1 + c_1(0)e^{-\Delta Et}}. \tag{11}$$

However, in most cases, 1-state fit is more conservative than two-state fit, thus we determine $\tilde{\psi}(L, b_\perp, z, P^z)$ by 1-state fit. Fig. (2) shows two examples.

For the LaMET approach to get the subtracted quasi-TMDWFs $\tilde{\psi}(b_\perp, z, P^z)$, the Wilson line between field operators in the matrix element in Eq. (7) is a staple link with the length L to the infinity, thus the L dependence of renormalized $C_2(L, b_\perp, z, t, P^z)$ need to be investigated. Fig. (3) shows an example of L dependence for renormalized $C_2(L, b_\perp, z, t, P^z)$ after 1-state fit for t. In addition, as we expected, the subtracted quasi-TMDWFs $\tilde{\psi}(b_\perp, z, P^z)$ are complex.

The curves of subtracted quasi-TMDWFs $\tilde{\psi}$ in Fig. (3) turn to plateaus when L is larger than 0.4fm, namely unsubtracted quasi-TMDWFs $\tilde{\psi}_l$ decays as the same speed as the square root of Wilson-loop $\sqrt{Z_E}$ for L. Based on this observation, we will use $L = 6a = 0.72$fm as asymptotic results to the infinity approach of L for all cases in the following calculation.

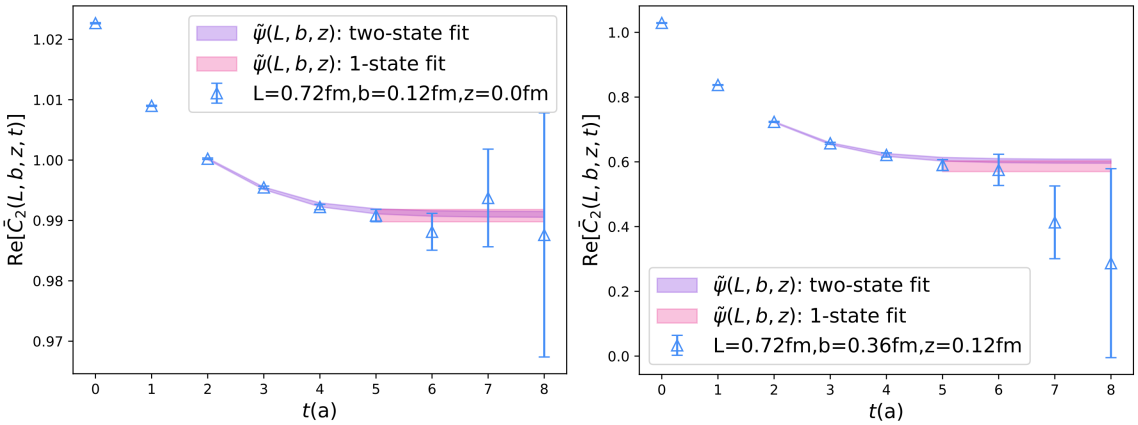

Figure 2: Examples of normalized two point correlation functions $\tilde{C}_2(L, b_\perp, z, t)$ defined in Eq. (11) performed as described below. The fit range for two-state fit is $t \sim [1a, 8a]$, which for 1-state fit is $t \sim [5a, 8a]$

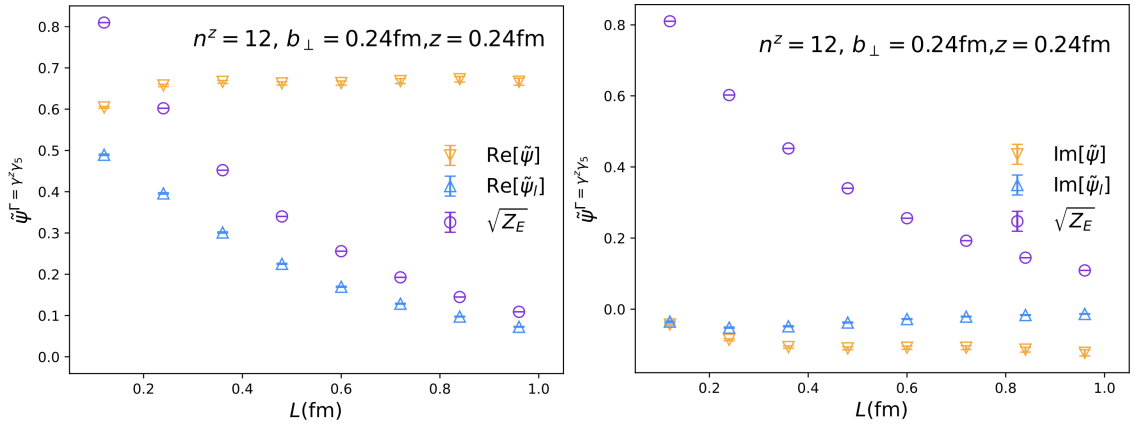

Figure 3: Results of L-dependence of the subtracted and unsubtracted quasi-TMDWFs ($\tilde{\psi}$ and $\tilde{\psi}_l$), and also the square root of the Wilson loop which is used for the subtraction. We take the $\{P^z, b_\perp, z\} = \{24\pi/L, 2a, 2a\}$ as an example.

As shown in Eq.(8), quark bilinear operators with staple-shaped Wilson lines are used to study the quasi-TMDWFs on lattice. In order to increase the signal of the calculation, we apply the leading twist operators $\bar{\Psi}(x)\gamma^\mu\gamma_5\Psi(y)$. The corresponding matrix element is proportional to the momentum of external state:

$$\langle 0|\bar{\Psi}(x)\gamma^\mu\gamma_5\Psi(y)|\pi(P)\rangle \propto i f_\pi P^\mu. \tag{12}$$

Due to the pion momentum set along z-direction, there are two different leading twist Lorentz structures, $\Gamma = \gamma^t\gamma_5$ and $\Gamma = \gamma^z\gamma_5$, which have identical contributions theoretically. We performed the subtracted quasi-TMDWFs in coordinate space $\tilde{\psi}(b_\perp, z, P^z)$ in Fig. (4), in which we compare the quasi-TMDWF $\tilde{\psi}(b_\perp, z, P^z)$ as the function of zP^z with $\Gamma = \gamma^z\gamma_5$ and $\gamma^t\gamma_5$ to investigate the difference of these two cases on lattice calculation. From the comparison we can see that the difference of these leading twist cases is not significant. It indicates that the higher twist terms make little contributions. So that we only adopt $\Gamma = \gamma^z\gamma_5$ for the following analysis. Additionally, we

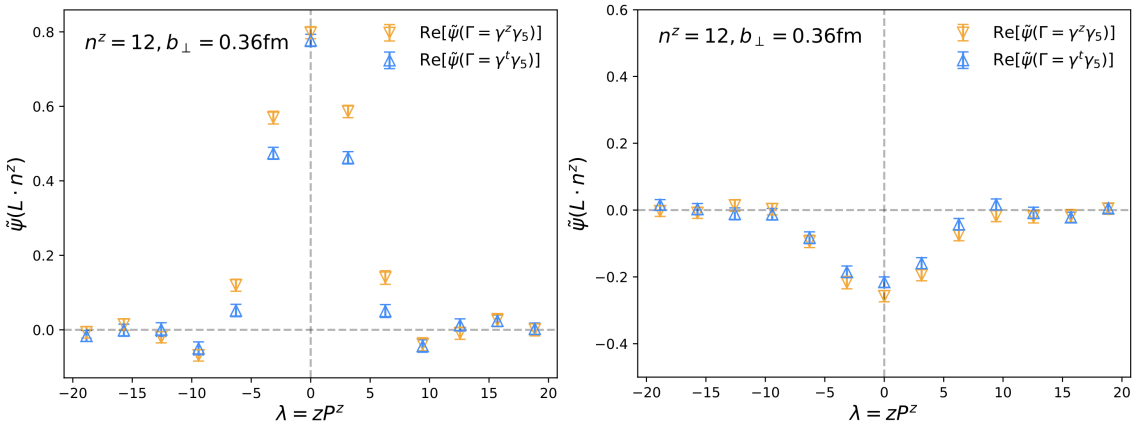

Figure 4: Examples of numerical results for $\tilde{\psi}(z, b_\perp, P^z)$ with $\{P^z, b\} = \{24\pi/L, 3a\}$.

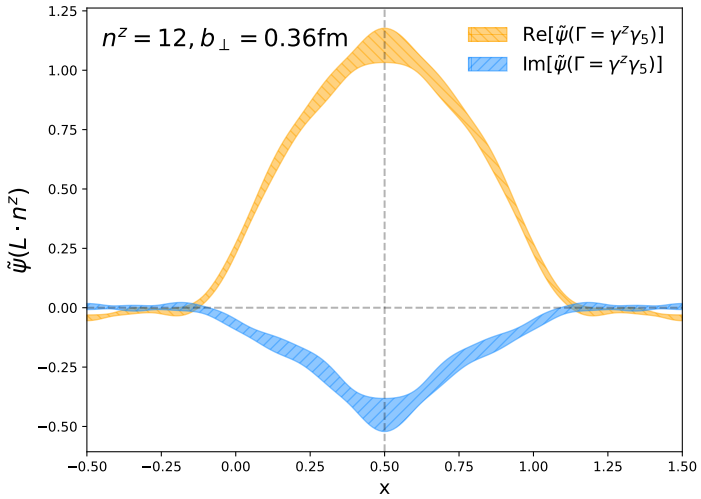

Figure 5: Numerical results for $\tilde{\psi}(b_\perp, x)$ with $\{P^z, b_\perp\} = \{24\pi/L, 3a\}$.

will compare the final results for Collins-Soper kernel $K(b_\perp, \mu)$ extracted from these two leading twist quasi-TMDWFs respectively to see if there is difference.

In order to get the quasi-TMDWFs in momentum space $\tilde{\psi}(b_\perp, x, P^z)$, we compute the Fourier transformation in Eq. (13)

$$\tilde{\psi}(b_\perp, x, P^z) = \int_{-\infty}^{\infty} \frac{P^z dz}{4\pi} e^{i(x-1/2)P^z z}\, \tilde{\psi}(b_\perp, x, P^z). \tag{13}$$

When $|z| \geq z_{max}$, $\tilde{\psi}(b_\perp, z, P^z)$ comes to zero with the statistical uncertainty as Fig. (4) shows, thus the limited data as z form $-z_{max}$ to z_{max} we have, we cut $z \to z_{max}$ to represent $z \to \infty$. We obtain the subtracted quasi-TMDWFs in momentum space $\tilde{\psi}(b_\perp, x, P^z)$. One example of $\tilde{\psi}(b_\perp, x, P^z)$ for $b = 0.36$fm is shown in Fig. (5), and we can see the imaginary part still exist, which is different from 1-dimensional wave functions[13].

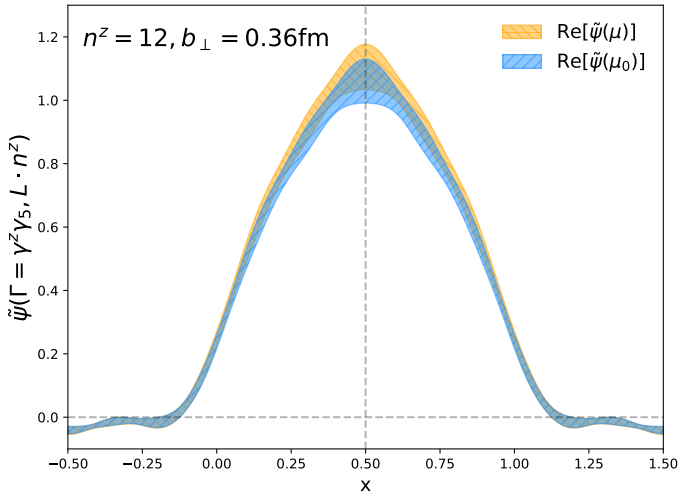

Figure 6: Comparison of numerical results for $\tilde{\psi}_{\rm Re}(x, b_\perp, \mu_0 = P^z, \zeta_z)$ and $\tilde{\psi}_{\rm Re}(x, b_\perp, \mu = 2\text{GeV}, \zeta_z)$. Take the case of $\{P^z, b_\perp\} = \{24\pi/L, 3a\}$ as a example.

Moreover, in order to match the $\overline{\rm MS}$ renormalization scheme, we need to consider the scale dependence of subtracted quasi-TMDWFs $\tilde{\psi}(b_\perp, x, P^z)$. For $\tilde{\psi}(b_\perp, x, P^z)$, the renormalization scale μ-dependence satisfies the renormalization group equation[4]:

$$\mu^2 \frac{d^2}{d\mu^2} \ln \tilde{\psi}_{\rm Re}(x, b_\perp, \mu, \zeta_z) = \gamma_F\left(\alpha_s(\mu)\right), \tag{14}$$

$$\mu^2 \frac{d^2}{d\mu^2} \ln \tilde{\psi}_{\rm Im}(x, b_\perp, \mu, \zeta_z) = 0. \tag{15}$$

For our calculation, the hadron momenta for three cases are $P^z = \{1.72, 2.15, 2.58\}$GeV, so we can evolute the results of $\tilde{\psi}(b_\perp, x, \mu_0 = P^z, P^z)$ to $\overline{\rm MS}$ scheme at $\mu = 2$GeV by Eq. (16)

$$\begin{aligned}
&\tilde{\psi}_{\rm Re}(b_\perp, x, \mu, P_z) = \tilde{\psi}_{\rm Re}(x, b_\perp, \mu_0, P_z) \times \exp \int_{\mu_0}^{\mu} \frac{4d\mu^2}{\beta_0 \mu^2 (\ln \mu^2 - \ln \Lambda^2)}, \\
&\tilde{\psi}_{\rm Im}(b_\perp, x, \mu_0, P_z) = \tilde{\psi}_{\rm Im}(b_\perp, x, \mu, P_z),
\end{aligned} \tag{16}$$

here we adopt the 1-loop result of $\alpha_s(\mu) = \frac{4\pi}{\beta_0 \ln \frac{\mu^2}{\Lambda^2}}$, $\beta_0 = 11 - \frac{2}{3}N_f$. The comparison of $\tilde{\psi}(b_\perp, x, \mu_0 = P^z, P^z)$ and $\tilde{\psi}(b_\perp, x, \mu, P^z)$ is performed in Fig. (6), which shows there's not much difference between subtracted quasi-TMDWFs at scale point $\mu_0 = 2.56$GeV and $\mu = 2$GeV. This scale dependence is related to Collins-Soper kernel. Due to the momenta we choose for the calculation are all around 2GeV, we may ignore the scale dependence between $\mu_0 = P^z$ and μ to extract Collins-Soper kernel.

Eq. (3) indicates that the Collins-Soper kernel can be extracted from the combination of $\tilde{\psi}^+$ and $\tilde{\psi}^-$ which is related to $\tilde{\psi}$. In principle, $K(b_\perp, \mu)$ does not have momentum fraction x-dependence, however, quasi-TMDWFs has the high order terms of $1/xP^z$ and $1/(1-x)P^z$, which dominate

when $x \sim 0, 1$. It influences $K(b_\perp, \mu)$ in the area $x \sim 0, 1$ by the following paramatization Eq. (17)

$$K(b_\perp, \mu, x, P_1^z, P_2^z) = K(b_\perp, \mu) + A\left[\frac{1}{x^2(1-x)^2(P_1^z)^2} - \frac{1}{x^2(1-x)^2(P_2^z)^2}\right]. \tag{17}$$

Therefore, we should eliminate the x-dependence by the fit of $K(b_\perp, \mu, x, P_1^z, P_2^z)$ as a function of x. Our data shows $K(b_\perp, \mu)$ is real to a high extent, so only this significantly non-zero real part is considered for this fit and the final result. The result of central value of $K(b_\perp, \mu)$ is generated by the average of bootstrap fit results, and the uncertainty is the standard deviation at 68% confidence interval of them. Our data shows the bootstrap joint fit can give the plateau of x for $K(b_\perp, \mu, x, P_1^z, P_2^z)$, and that of different momentum combinations are not all that dissimilar.

In addition, as a comparison, the tree level result of $K(b_\perp, \mu)$ is computed by coordinate quasi-TMDWFs $\tilde{\psi}(b, z, P^z, \mu)$, in which $H_1^\pm = 1$

$$K_0(b_\perp, \mu) = \frac{1}{2}\left(\frac{1}{\ln(P_1^z/P_2^z)} \ln \frac{\tilde{\psi}^+(b_\perp, z=0, \mu, P_1^z)}{\tilde{\psi}^+(b_\perp, z=0, \mu, P_2^z)} + \frac{1}{\ln(P_1^z/P_2^z)} \ln \frac{\tilde{\psi}^-(b_\perp, z=0, \mu, P_1^z)}{\tilde{\psi}^-(b_\perp, z=0, \mu, P_2^z)}\right). \tag{18}$$

Also, the systematical uncertainty needs to be considered to determine the final result $K(b_\perp, \mu)$. It is formed as the following equation Eq. (19).

$$\sigma_{sys} = \sqrt{K(b_\perp, \mu) + \mathrm{Im}^2[K^+(b_\perp, \mu)]} - K(b_\perp, \mu), \tag{19}$$

$K(b_\perp, \mu)$ is related to the $K(b_\perp, \mu)$ extracted from the average of $\tilde{\psi}^+$ and $\tilde{\psi}^-$. The imaginary part of $K(b_\perp, \mu)$ is ignored. $\mathrm{Im}[K^+(b_\perp, \mu)]$ represents the numerical imaginary part of extracting $K(b_\perp, \mu)$ only by $\tilde{\psi}^+$ in the following equation Eq. (20)

$$K^+(b_\perp, \mu) = \frac{1}{\ln(P_1^z/P_2^z)} \ln \frac{\tilde{\psi}_N^+(x, b_\perp, \mu, P_1^z)}{\tilde{\psi}_N^+(x, b_\perp, \mu, P_2^z)}. \tag{20}$$

We compared this result with previous Lattice QCD results and perturbative calculations in Fig. (7), which shows in small $b_\perp$ area. Our result reaching to one loop matching kernel for TMDWFs is very close to the perturbative calculation. Besides, our results are consistent with others', and are more precise in large $b_\perp$ area.

4. Summary and Outlook

We have computed the Collins-Soper kernel as a function of the transverse seperation $b_\perp$, which is extracted from quasi-TMDWFs up to 1-loop matching kernel on lattice in LaMET approach. We have given the figures of quasi-TMDWFs as a function of momentum fraction x at fixed points $b_\perp = b_f$. We have investigated the x-dependence for Collins-Soper kernel through a 2-parameter fit. Our results are consistent with previously Lattice QCD calculations. According to our plan, in a near future, we will make the x-dependence fit more accurate and add some of phenomenological results based on Drell-Yan data.

Further, compared with most former Collins-Soper kernel calculations, the uncertainty of our results is smaller, especially in the large $b_\perp$ area. Our calculation is the first attempt to extract Collin-Soper kernel from quasi-TMDWFs up to 1-loop matching kernel. This has added evidences for the extraction of partonic structure from LQCD in LaMET.

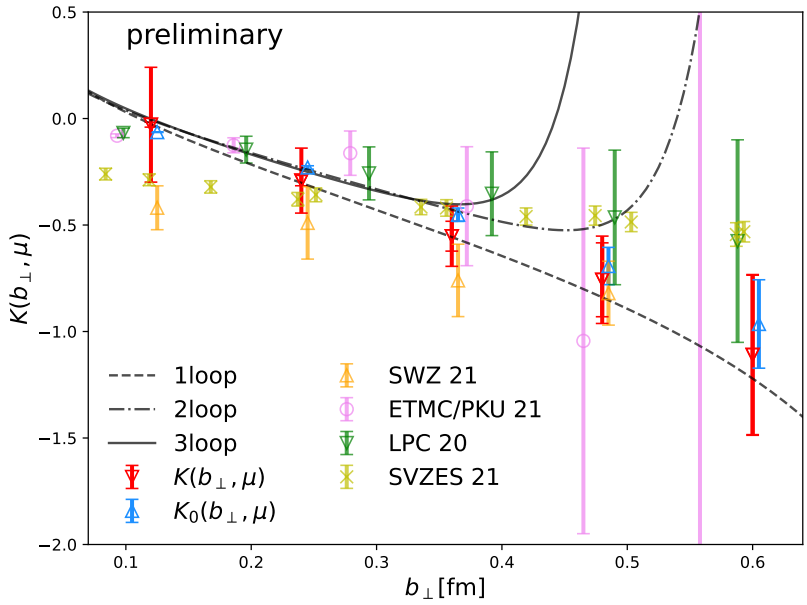

Figure 7: This is the preliminary results for $K(b_\perp,\mu)$, compared with SWZ[14], LPC collaborations[10] as well as ETMC/PKU[12], SVZES[11] and the perturbative calculations (at small $b_\perp$) with the strong coupling α_s up to three loop are also shown. Statistical and systematic errors have been added in quadrature.

Acknowledgement

I thank Jun Hua, Xiangdong Ji, Andreas Schäfer, Peng Sun, Wei Wang, Yibo Yang, Jian-Hui Zhang, and Qi-An Zhang for the collaboration. This work is supported in part by Natural Science Foundation of China under grant No. 11735010, 11911530088, U2032102, also supported by Natural Science Foundation of Shanghai under grant No. 15DZ2272100.

References

[1] X. Ji, Phys. Rev. Lett. **110**, 262002 (2013) doi:10.1103/PhysRevLett.110.262002 [arXiv:1305.1539 [hep-ph]].

[2] X. Ji, Sci. China Phys. Mech. Astron. **57**, 1407-1412 (2014) doi:10.1007/s11433-014-5492-3 [arXiv:1404.6680 [hep-ph]].

[3] K. Cichy and M. Constantinou, Adv. High Energy Phys. **2019**, 3036904 (2019) doi:10.1155/2019/3036904 [arXiv:1811.07248 [hep-lat]].

[4] X. Ji, Y. S. Liu, Y. Liu, J. H. Zhang and Y. Zhao, Rev. Mod. Phys. **93**, no.3, 035005 (2021) doi:10.1103/RevModPhys.93.035005 [arXiv:2004.03543 [hep-ph]].

[5] X. Ji, Y. Liu and Y. S. Liu, Nucl. Phys. B **955**, 115054 (2020) doi:10.1016/j.nuclphysb.2020.115054 [arXiv:1910.11415 [hep-ph]].

[6] X. Ji, Y. Liu and Y. S. Liu, Phys. Lett. B **811**, 135946 (2020) doi:10.1016/j.physletb.2020.135946 [arXiv:1911.03840 [hep-ph]].

[7] M. A. Ebert, I. W. Stewart and Y. Zhao, JHEP **09**, 037 (2019) doi:10.1007/JHEP09(2019)037 [arXiv:1901.03685 [hep-ph]].

[8] X. Ji and Y. Liu, [arXiv:2106.05310 [hep-ph]].

[9] P. Shanahan, M. Wagman and Y. Zhao, Phys. Rev. D **102**, no.1, 014511 (2020) doi:10.1103/PhysRevD.102.014511 [arXiv:2003.06063 [hep-lat]].

[10] Q. A. Zhang *et al.* [Lattice Parton], Phys. Rev. Lett. **125**, no.19, 192001 (2020) doi:10.1103/PhysRevLett.125.192001 [arXiv:2005.14572 [hep-lat]].

[11] M. Schlemmer, A. Vladimirov, C. Zimmermann, M. Engelhardt and A. Schäfer, JHEP **08**, 004 (2021) doi:10.1007/JHEP08(2021)004 [arXiv:2103.16991 [hep-lat]].

[12] Y. Li, S. C. Xia, C. Alexandrou, K. Cichy, M. Constantinou, X. Feng, K. Hadjiyiannakou, K. Jansen, C. Liu and A. Scapellato, *et al.* [arXiv:2106.13027 [hep-lat]].

[13] J. Hua *et al.* [Lattice Parton], Phys. Rev. Lett. **127**, no.6, 062002 (2021) doi:10.1103/PhysRevLett.127.062002 [arXiv:2011.09788 [hep-lat]].

[14] P. Shanahan, M. Wagman and Y. Zhao, [arXiv:2107.11930 [hep-lat]].

[15] E. Follana *et al.* [HPQCD and UKQCD], Phys. Rev. D **75**, 054502 (2007) doi:10.1103/PhysRevD.75.054502 [arXiv:hep-lat/0610092 [hep-lat]].

[16] A. Bazavov *et al.* [MILC], Phys. Rev. D **87**, no.5, 054505 (2013) doi:10.1103/PhysRevD.87.054505 [arXiv:1212.4768 [hep-lat]].

PoS(LATTICE2021)424